ISSN 1070-4280, Russian Journal of Organic Chemistry, 2020, Vol. 56, No. 7, pp. 1279–1288. © Pleiades Publishing, Ltd., 2020.

Nano-ZnO Impregnated on Starch—A Highly Efficient Heterogeneous Bio-Based Catalyst for One-Pot Synthesis of Pyranopyrimidinone and Xanthene Derivatives as Potential Antibacterial Agents

A. Amininia[a], K. Pourshamsian[a,*], and B. Sadeghi[a]

[a] *Department of Chemistry, Tonekabon Branch, Islamic Azad University, Tonekabon, 46841-61167 Iran*

**e-mail: Kshams49@gmail.com*

Received January 25, 2020; revised February 5, 2020; accepted February 11, 2020

Abstract—A new method has been proposed for the synthesis of pyranopyrimidinone and xanthene derivatives using zinc oxide–starch nanocomposite as catalyst under microwave irradiation. The ZnO–starch nanocomposite was characterized by X-ray diffraction and scanning electron microscopy data, and the size of the ZnO-starch nanocomposite particles was estimated at 70–90 nm. The catalyst was used in the three-component condensation of aromatic aldehydes with barbituric acid and malononitrile and the 1:2 condensation of aromatic aldehydes with naphthalen-2-ol to obtain pyranopyrimidinone and xanthene derivatives, respectively. The catalyst can be reused several times without loss of catalytic activity. The proposed procedure utilizes affordable and inexpensive materials, provides excellent yields in short reaction time, and is eco-friendly, which makes it more economic than conventional methods. The antibacterial activity of the synthesized compounds was evaluated against *M. luteus* and *P. aeruginosa*.

Keywords: ZnO–starch nanocomposite, microwave-assisted synthesis, pyranopyrimidinone, xanthene, antibacterial activity

DOI: 10.1134/S1070428020070234

INTRODUCTION

Pyranopyrimidinone and xanthene derivatives constitute important classes of organic compounds used in pharmaceutical chemistry [1]. They have various pharmacological activities such as antiviral [2], antibacterial [3], antitumor [4], hepatoprotective [5], antifungal [6], and anti-inflammatory activities [7] and are used as food additives [8]. Several synthetic protocols have been reported for the synthesis of pyranopyrimidinone and xanthene derivatives, including cyclizations catalyzed by palladium compounds [9–11], various Lewis acids such as $NbCl_2$ [12–14], and Brønsted acids [15–18].

Many of the reported methods for synthesis of the pyranopyrimidinone and xanthene derivatives utilize expensive reagents and catalysts, strongly acidic conditions, inert atmosphere, and toxic organic solvents and are characterized by long reaction times and low yields [19–21]. In order to avoid these restrictions, the development of new highly effective catalysts and environmentally benign procedures is essential for the synthesis of pyranopyrimidinone and xanthene derivatives.

Many organic reactions are carried out at elevated temperature on heating on an oil or sand bath. These old methods can cause problems such as by-product formation, product decomposition, and so on. Microwave heating, in addition to solving these problems, provides very rapid reactions and generates a heat system that cannot be easily accessed by other methods [22, 23]. The main advantage of using microwave radiation in the synthesis of organic compounds is much shorter reaction time than in conventional thermal method.

In continuation of our research aimed at finding efficient catalysts for the synthesis of pyranopyrimidinone and xanthene, we focused on another suitable substrate for the synthesis of nanocomposite catalysts. Such a substrate is starch which is an affordable, inexpensive, and environmentally friendly material.

RESULTS AND DISCUSSION

We were interested in the synthesis of pyrano-[2,3-*d*]pyrimidine and xanthene derivatives via a domino Knoevenagel–Michael condensation [24–29] catalyzed by ZnO&starch in aqueous ethanol under microwave irradiation at a power of 230 W. The catalytic significance of ZnO&starch has been highlighted in increasing the yield of the products. The catalyst was prepared according to the reported procedure [30].

Previous investigations have shown that Lewis acids reduce the potential barrier to reactions. We decided to investigate the catalytic activity of ZnO–starch nanocomposite, which can act as a Lewis acid because of its empty orbitals. In recent years, a variety of polymers have been studied as lightweight matrices for coating and modifying nanoparticles [31]. In addition, the polymer shell inhibits nanoparticle aggregation, increases stability, reduces toxicity, and increases shelf life [32]. According to [33], the viscosity of water and starch is high. By adding a solution of zinc salt a solution with lower viscosity is obtained. Presumably, zinc ions interact with hydroxy oxygen atoms of starch, thus weakening the intermolecular hydrogen bonding of the starch and disrupting its crystalline structure, which gives a solution with lower viscosity.

The morphology of ZnO&St nanocomposite was investigated by scanning electron microscopy. Figure 1a

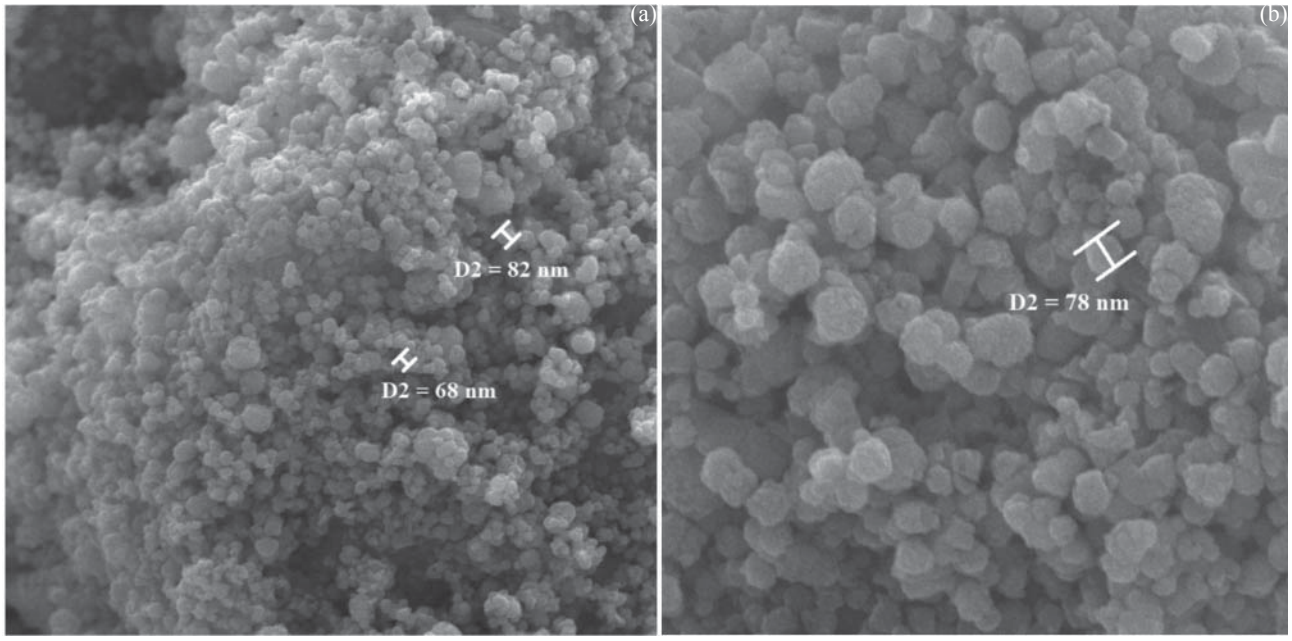

Fig. 1. SEM images of ZnO&St nanocomposite at different magnifications: (a) view field 2.97 μm; (b) view field 10.9 μm.

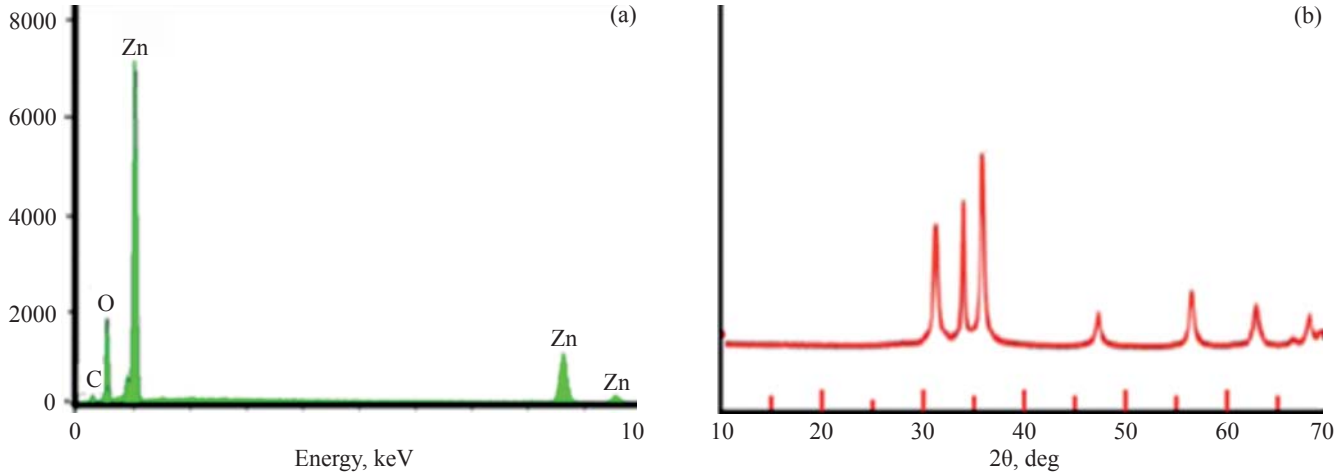

Fig. 2. (a) EDX and (b) XRD patterns of ZnO&St.

Scheme 1.

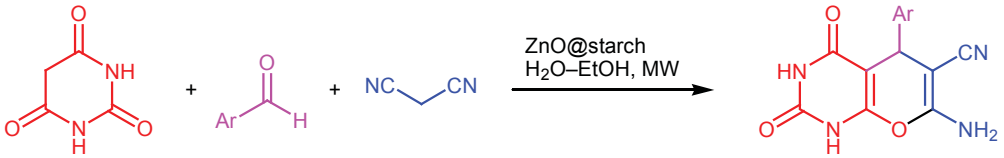

1 **2** **3** **4a–4i**

4, Ar = 4-BrC_6H_4 (**a**), 3-ClC_6H_4 (**b**), 2-ClC_6H_4 (**c**), 2,3-$Cl_2C_6H_4$ (**d**), 4-NCC_6H_4 (**e**), 2,4-$Cl_2C_6H_4$ (**f**), 3-HOC_6H_4 (**g**), 4-$O_2NC_6H_4$ (**h**), 4-$F_3CC_6H_4$ (**i**).

Scheme 2.

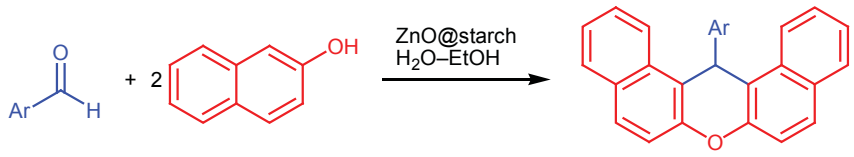

2 **5** **6a–6k**

6, Ar = 2,4-$Cl_2C_6H_4$ (**a**), 3-$MeOC_6H_4$ (**b**), Ph (**c**), 4-BrC_6H_4 (**d**), 3-$O_2NC_6H_4$ (**e**), 3-MeC_6H_4 (**f**), 4-ClC_6H_4 (**g**), 4-$MeOC_6H_4$ (**h**), 3-ClC_6H_4 (**i**), 3-BrC_6H_4 (**j**), 4-FC_6H_4 (**k**).

shows that the ZnO&St particles are spherical in shape with an average size of 75 nm. The SEM image at higher magnification completely confirmed the information obtained from the catalytic morphology (Fig. 1b). The chemical purity of ZnO&St samples was checked by energy-dispersive X-ray spectroscopy (EDX). The X-ray diffraction pattern (XRD) of ZnO&St is shown in Fig. 2. The obtained pattern corre-

Table 1. Synthesis of pyranopyrimidine **4a** in the presence of ZnO–starch nanocomposite under different conditions

Catalyst amount, mg	Solvent	Temperature conditions	Reaction time, min	Yield, %
2	H_2O	MW	10	–
5	H_2O	MW	10	33
7	H_2O	MW	10	54
10	H_2O	MW	10	72
15	H_2O	MW	10	75
20	H_2O	MW	10	80
22	H_2O	MW	10	86
25	H_2O	MW	10	87
30	H_2O	MW	10	89
22	EtOH	MW	10	89
22	DMF	MW	10	65
22	CH_2Cl_2	MW	10	72
22	**EtOH/H_2O (1/1)**	**MW**	**10**	**94**
22	H_2O	Reflux	45	90
22	EtOH/H_2O (1/1)	Reflux	25	77
22	EtOH/H_2O (1/1)	Reflux	35	81
22	EtOH/H_2O (1/1)	Reflux	45	87
22	EtOH/H_2O (1/1)	Reflux	60	92
22	No solvent	MW	60	38

Table 2. Synthesis of xanthene **6c** in the presence of ZnO–starch nanocomposite under different conditions

Catalyst amount, mg	Solvent	Temperature conditions	Reaction time, min	Yield, %
5	H_2O	MW	15	38
10	H_2O	MW	15	57
15	H_2O	MW	15	71
20	H_2O	MW	15	78
25	H_2O	MW	15	89
30	H_2O	MW	15	90
35	H_2O	MW	15	91
30	EtOH	MW	15	85
30	DMF	MW	15	65
30	CH_2Cl_2	MW	15	72
30	**EtOH/H_2O (1/1)**	**MW**	**15**	**92**
30	H_2O	Reflux	45	90
30	EtOH/H_2O (1/1)	Reflux	25	67
30	EtOH/H_2O (1/1)	Reflux	35	74
30	EtOH/H_2O (1/1)	Reflux	45	87
30	EtOH/H_2O (1/1)	Reflux	60	92
30	Solvent free	MW	60	38

sponds to the hexagonal (wurtzite) crystal structure of the nanocatalyst. These results confirmed the presence of ZnO in ZnO&St.

The ZnO&St nanocomposite was used to catalyze the three-component condensation of barbituric acid (**1**) with aromatic aldehydes **2** and malononitrile (**3**) to obtain pyranopyrimidine derivatives **4a**–**4i** (Scheme 1), as well as the 1:2 condensation of aromatic aldehydes **2** with naphthalen-2-ol (**5**) to produce xanthenes **6a**–**6k** (Scheme 2). The model reactions were performed under various conditions with variation of the solvent (water, ethanol, dimethylformamide, methylene chloride, 1:1 aqueous ethanol, and solvent-free) at different temperature conditions (reflux or microwave irradiation) with different amounts of the catalyst and different reaction times (Tables 1, 2). The results showed that the product yield was higher in protic solvents, and

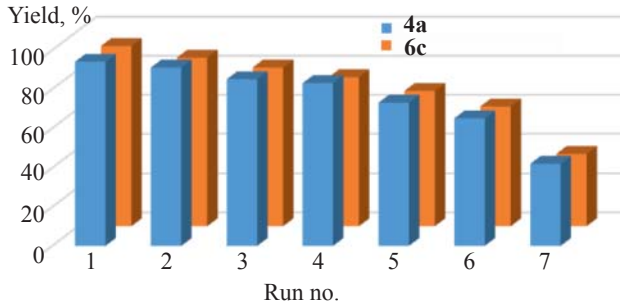

Fig. 3. Reusability of ZnO&St in the synthesis of pyranopyrimidinone **4a** and xanthene **6c**.

the best yields were obtained in aqueous ethanol at a ratio of 1:1. The amount of the catalyst was varied from 2 to 35 mg. It was found that the catalyst amount 22 mg in the synthesis of **4a** and 30 mg in the synthesis of **7c** provided the highest product yields. Further increase of the catalyst amount did not lead to a significant increase in the yield. The optimal reaction conditions are highlighted in bold red in Tables 1 and 2.

Thus, the use of ZnO&St nanocomposite together with microwave irradiation significantly accelerated the reactions and provided good yields and simple workup in the preparation of pyranopyrimidinone and xanthene derivatives.

Plausible catalytic mechanisms for both reactions are depicted in Scheme 3. In the synthesis of pyranopyrimidinone derivatives, yellowish arylidenemalononitrile was initially formed via Knoevenagel condensation of malononitrile and activated aromatic aldehyde in quantitative yield. The subsequent Michael addition, followed by intramolecular cyclization, afforded the final product.

Various aromatic aldehydes reacted with malononitrile and barbituric acid in the synthesis of pyranopyrimidinone derivatives and with β-naphtol in the synthesis of xanthene derivatives under the optimized conditions to give the corresponding products in high yields and in short reaction times. The obtained results are summarized in Tables 3 and 4.

Scheme 3.

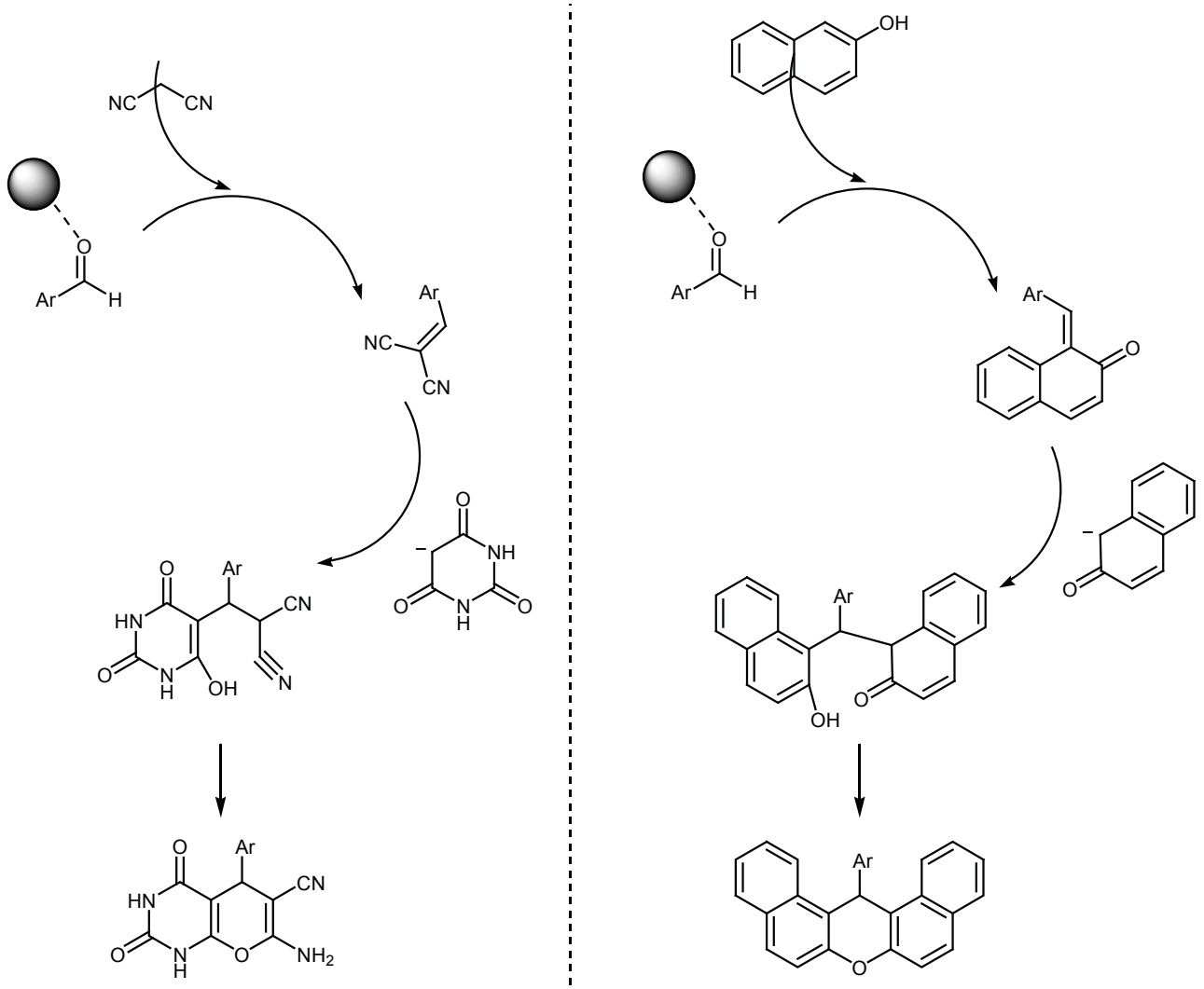

Table 3. Reaction times, yields, and melting points of compounds **4a**–**4i**

Compound no.	Ar	Reaction time, min	Yield, %	Melting point, °C		Reference
				reported	found	
4a	4-BrC_6H_4	12	91	230–231	235–237	[34]
4b	3-ClC_6H_4	13	92	240–241	245–247	[34]
4c	2-ClC_6H_4	14	85	240–241	247–249	[34]
4d	2,3-$Cl_2C_6H_4$	19	81	240–242	250–251	[35]
4e	4-NCC_6H_4	11	95	254–256	265–266	[35]
4f	2,4-$Cl_2C_6H_4$	18	85	241–242	238–239	[36]
4g	3-HOC_6H_4	17	90	158–160	165–166	[36]
4h	4-$O_2NC_6H_4$	11	91	239–240	241–242	[36]
4i	4-$F_3CC_6H_4$	12	93	250–251	260–261	[36]

Table 4. Reaction times, yields, and melting points of compounds **6a**–**6k**

Compound no.	Ar	Reaction time, min	Yield, %	Melting point, °C		Reference
				found	reported	
6a	2,4-$Cl_2C_6H_4$	14	88	251–252	255–257	[37]
6b	3-$MeOC_6H_4$	15	91	181–183	179–181	[37]
6c	Ph	12	92	184–185	187–189	[37]
6d	4-BrC_6H_4	17	88	303–305	310–312	[37]
6e	3-$O_2NC_6H_4$	17	95	213–215	217–220	[38]
6f	3-MeC_6H_4	11	95	197–200	190–192	[39]
6g	4-ClC_6H_4	14	90	288–290	295–297	[40]
6h	4-$MeOC_6H_4$	13	89	215–217	219–221	[40]
6i	3-ClC_6H_4	14	88	217–220	225–227	[40]
6j	3-BrC_6H_4	12	85	198–200	201–202	[41]
6k	4-FC_6H_4	15	89	255–258	265–266	[41]

Table 5. In vitro antibacterial activity of compounds **4a**–**4i** and **6a**–**6k** against *M. luteus*

Compound no.	Concentration, μg/mL						MBC, μg/mL
	2000	1000	500	250	125	62.5	
4a	Inhibition	Inhibition	Inhibition	Inhibition	Growth	Growth	250
4b	Inhibition	Inhibition	Inhibition	Inhibition	Growth	Growth	250
4c	Inhibition	Inhibition	Inhibition	Inhibition	Growth	Growth	250
4d	Inhibition	Inhibition	Inhibition	Inhibition	Growth	Growth	250
4e	Inhibition	Inhibition	Inhibition	Inhibition	Growth	Growth	250
4f	Inhibition	Inhibition	Inhibition	Inhibition	Growth	Growth	250
4g	Inhibition	Inhibition	Inhibition	Inhibition	Growth	Growth	250
4h	Inhibition	Inhibition	Inhibition	Inhibition	Growth	Growth	250
4i	Inhibition	Inhibition	Inhibition	Inhibition	Growth	Growth	250
6a	Inhibition	Inhibition	Inhibition	Growth	Growth	Growth	500
6b	Inhibition	Inhibition	Inhibition	Growth	Growth	Growth	500
6c	Inhibition	Inhibition	Inhibition	Growth	Growth	Growth	500
6d	Inhibition	Inhibition	Inhibition	Growth	Growth	Growth	500
6e	Inhibition	Inhibition	Inhibition	Growth	Growth	Growth	500
6f	Inhibition	Inhibition	Inhibition	Growth	Growth	Growth	500
6g	Inhibition	Inhibition	Inhibition	Growth	Growth	Growth	500
6h	Inhibition	Inhibition	Inhibition	Growth	Growth	Growth	500
6i	Inhibition	Inhibition	Inhibition	Growth	Growth	Growth	500
6j	Inhibition	Inhibition	Inhibition	Growth	Growth	Growth	500
6k	Inhibition	Inhibition	Inhibition	Growth	Growth	Growth	500
Tetracycline	Inhibition	Inhibition	Inhibition	Inhibition	Inhibition	Inhibition	< 62.5

One of the most important features of a solid catalyst is its recyclability. The recyclability of ZnO&St NCs was investigated using the model reaction. After completion of the reaction, the catalyst was filtered off, washed well with acetone and ethyl acetate, and used in the next reaction cycle. The results showed that the catalyst retained its activity after three runs (Fig. 3).

All the synthesized compounds were evaluated for their in vitro antibacterial activity against *Micrococcus luteus* (*M. luteus*) and *Pseudomonas aeruginosa* (*P. aeruginosa*) by determining their minimum inhibitory (MIC) and minimum bactericidal concentrations (MBC) in comparison to tetracycline used as standard drug. All the synthesized compounds showed good

Table 6. In vitro antibacterial activity (MBC, μg/mL) of compounds **4a**–**4i** and **6a**–**6k** against *P. aeruginosa*

Compound no.	Concentration, μg/mL						MBC, μg/mL
	2000	1000	500	250	125	62.5	
4a	Inhibition	Inhibition	Inhibition	Growth	Growth	Growth	500
4b	Inhibition	Inhibition	Inhibition	Growth	Growth	Growth	500
4c	Inhibition	Inhibition	Inhibition	Growth	Growth	Growth	500
4d	Inhibition	Inhibition	Growth	Growth	Growth	Growth	1000
4e	Inhibition	Inhibition	Growth	Growth	Growth	Growth	1000
4f	Inhibition	Inhibition	Growth	Growth	Growth	Growth	1000
4g	Inhibition	Inhibition	Growth	Growth	Growth	Growth	1000
4h	Inhibition	Inhibition	Growth	Growth	Growth	Growth	1000
4i	Inhibition	Inhibition	Growth	Growth	Growth	Growth	1000
6a	Inhibition	Inhibition	Growth	Growth	Growth	Growth	1000
6b	Inhibition	Inhibition	Growth	Growth	Growth	Growth	1000
6c	Inhibition	Inhibition	Growth	Growth	Growth	Growth	1000
6d	Inhibition	Inhibition	Growth	Growth	Growth	Growth	1000
6e	Inhibition	Inhibition	Growth	Growth	Growth	Growth	1000
6f	Inhibition	Inhibition	Growth	Growth	Growth	Growth	1000
6g	Inhibition	Inhibition	Growth	Growth	Growth	Growth	1000
6h	Inhibition	Inhibition	Growth	Growth	Growth	Growth	1000
6i	Inhibition	Inhibition	Inhibition	Growth	Growth	Growth	500
6j	Inhibition	Inhibition	Inhibition	Growth	Growth	Growth	500
6k	Inhibition	Inhibition	Inhibition	Growth	Growth	Growth	500
Tetracycline	Inhibition	Inhibition	Inhibition	Inhibition	Inhibition	Inhibition	< 62.5

antibacterial activity. Pyranopyrimidinone derivatives **4a**–**4i** were generally more active than xanthenes **6a**–**6k** (Tables 5, 6).

In conclusion, we have proposed a convenient and efficient procedure for the synthesis of pyranopyrimidine and xanthene derivatives in the presence of ZnO&St nanocomposite under microwave irradiation. The procedure is advantageous due to short reaction time, low cost, simple operation, and recyclability of the catalyst. In many cases, the products crystallized directly from the reaction mixture in high purity.

EXPERIMENTAL

The chemicals and solvents (all of analytical grade) used in the synthesis of pyranopyrimidine and xanthene derivatives were obtained from Merck and Aldrich. The progress of reactions was monitored by thin-layer chromatography on 0.2-mm silica gel F-252 plates (Merck). The melting points were determined in open capillaries using an Electrothermal 9100 melting point apparatus and are uncorrected. The ^{1}H and ^{13}C NMR spectra were recorded on a Bruker 3000 spectrometer (400 and 100 MHz, respectively) using $CDCl_3$–DMSO-d_6 as solvent and tetramethylsilane as internal standard. The catalyst was prepared using a Tecno-Gaz Astra 3D ultrasound device (9.5 L, frequency 45 kHz, 305 W input power with heating, 2 transducers). All microwave-assisted reactions were carried out in a microwave oven.

Preparation of ZnO–starch nanocomposite. A reaction vessel was charged with 40 mL of distilled water, 0.2 g of starch and 1.2 g (4 mmol) of $ZnNO_3 \cdot 6H_2O$ were added, and the mixture was heated under ultrasound irradiation (20 kHz) at 40°C for 5 min. The mixture was then adjusted to pH 9 by adding dropwise a dilute solution of sodium hydroxide and ultrasonically irradiated for 15 min more. The white precipitate of ZnO&St was separated by centrifugation, washed several times with deionized water to remove impurities, and dried at 70°C for 24 h.

General procedure for the preparation of pyranopyrimidines 4a–4i. A mixture of aromatic aldehyde **2** (1 mmol), malononitrile (1.2 mmol, ~80 mg), barbituric acid (1 mmol, 156 mg), and 22 mg of ZnO&St in

aqueous ethanol (2 mL + 2mL) was irradiated in a microwave oven at a power of 230 W. After completion of the reaction, the resulting solid (crude product) was filtered off and recrystallized from ethanol. The physical data (melting points and NMR and IR spectra) of the known compounds were found to be identical with those reported in the literature. Spectral data for selected compounds are given below.

7-Amino-5-(3-chlorophenyl)-2,4-dioxo-1,3,4,5-tetrahydro-2*H*-pyrano[2,3-*d*]pyrimidine-6-carbonitrile (4b). Dark yellow powder, mp 240–241°C. IR spectrum (KBr), ν, cm^{-1}: 3419, 3300 (NH_2), 3186 (NH), 2192 (C≡N), 1689, 1654 (C=O). ^{1}H NMR spectrum, δ, ppm: 4.47 s (1H, 5-H), 7.28 br.s (2H, H_{arom}, NH_2), 7.61 t (1H, ^3J = 7.6 Hz, H_{arom}), 7.74 d (1H, ^3J = 7.6 Hz, H_{arom}), 8.06 br.s (1H, H_{arom}), 8.08–8.13 m (1H, H_{arom}), 11.11 s (1H, NH), 12.16 br.s (1H, NH).

7-Amino-5-(2-chlorophenyl)-2,4-dioxo-1,3,4,5-tetrahydro-2*H*-pyrano[2,3-*d*]pyrimidine-6-carbonitrile (4c). Dark yellow powder, mp 240–241°C. IR spectrum (KBr), ν, cm^{-1}: 3410, 3370 (NH_2), 3158 (NH), 2185 (C≡N), 1689 (C=O). ^{1}H NMR spectrum, δ, ppm: 4.72 s (1H, 5-H), 7.153 br.s (2H, NH_2), 7.21–7.28 m (3H, H_{arom}), 7.36 d (1H, H_{arom}), 11.06 s (1H, NH), 12.08 br.s (1H, NH).

7-Amino-5-(4-nitrophenyl)-2,4-dioxo-1,3,4,5-tetrahydro-2*H*-pyrano[2,3-*d*]pyrimidine-6-carbonitrile (4h). White powder, mp 239–240°C. IR spectrum (KBr), ν, cm^{-1}: 3477, 3238 (NH_2), 3127 (NH), 2192 (C≡N), 1677, 1645 (C=O). ^{1}H NMR spectrum, δ, ppm: 4.42 s (1H, 5-H), 7.21 br.s (2H, NH_2), 7.52 d (2H, ^3J = 8.8 Hz, H_{arom}), 8.16 d (2H, ^3J = 8.8 Hz, H_{arom}), 11.12 br.s (1H, NH), 12.17 br.s (1H, NH).

General procedure for the synthesis of xanthene derivatives 6a–6k. A reaction vessel was charged with water (5 mL) and ethanol (5 mL), 288 mg of naphthalen-2-ol (**5**, 2 mmol), benzaldehyde **2** (1 mmol), and 30 mg of ZnO&St were added, and the mixture was irradiated in a microwave oven at a power of 230 W. The progress of the reaction was monitored by TLC. After completion of the reaction, the mixture was cooled to room temperature, the catalyst was separated by filtration, the filtrate was evaporated, and the crude product was purified by recrystallization from ethanol. All products were characterized by comparison of their melting points and FT-IR spectra with published data. Spectral data of selected compounds are given below.

14-Phenyl-14*H*-dibenzo[*a*,*j*]xanthene (6c). White solid, mp 184–185°C. IR spectrum (KBr), ν, cm^{-1}: 3069, 3041, 2927, 1614, 1581, 1508, 1474, 1361. ^{1}H NMR spectrum, δ, ppm: 6.53 s (1H, 14-H), 7.04 t (1H, J = 7.2 Hz, H_{arom}), 7.18 t (2H, J = 7.2 Hz, H_{arom}), 7.45 t (2H, J = 7.5 Hz, H_{arom}), 7.53–7.60 m (6H, H_{arom}), 7.62 t (4H, J = 8 Hz, H_{arom}), 8.44 d (2H, J = 8 Hz, H_{arom}).

14-(3-Methylphenyl)-14*H*-dibenzo[*a*,*j*]xanthene (6f). Yellow solid, mp 197–200°C. IR spectrum (KBr), ν, cm^{-1}: 3018, 2921, 1623, 1591, 1512, 1457,1400, 1249, 960, 806, 806, 743. ^{1}H NMR spectrum, δ, ppm: 2.07 s (3H, CH_3), 6.67 s (1H, 14-H), 6.77 d (1H, J = 7.6 Hz, H_{arom}), 7.04 t (1H, J = 7.6 Hz, H_{arom}), 7.31 s (1H, H_{arom}), 7.45 m (2H, H_{arom}), 7.54 s (1H, H_{arom}), 7.56 d (2H, J = 8.8 Hz, H_{arom}), 7.63 m (2H, H_{arom}), 7.91–7.94 m (4H, H_{arom}), 8.67 d (2H, J = 8.4 Hz, H_{arom}).

14-(4-Methoxyphenyl)-14*H*-dibenzo[*a*,*j*]xanthene (6h). White solid, mp 215–217°C. IR spectrum (KBr), ν, cm^{-1}: 3072, 2834, 1622, 1592, 1509, 1458, 1438, 1399, 1249, 1082. ^{1}H NMR spectrum, δ, ppm: 3.38 s (3H, CH_3), 6.68 s (1H, 14-H), 6.69 d (2H, J = 8.4 Hz, H_{arom}), 7.46 t (2H, J = 7.2 Hz, H_{arom}), 7.53 t (4H, J = 7.5 Hz, H_{arom}), 7.62 t (2H, H_{arom}), 7.93 t (4H, J = 8.4 Hz, H_{arom}), 8.66 d (2H, J = 8.4 Hz, H_{arom}).

14-(3-Chlorophenyl)-14*H*-dibenzo[*a*,*j*]xanthene (6i). White solid, mp 217–220°C. IR spectrum (KBr), ν, cm^{-1}: 3467, 3057, 1658, 1622, 1591, 1514, 1473, 1458, 1431, 1400, 1240, 1238. ^{1}H NMR spectrum, δ, ppm: 6.73 s (1H, 14-H), 7.00 t (1H, J = 8.4 Hz, H_{arom}), 7.07 t (1H, J = 7.2 Hz, H_{arom}), 7.31 d (1H, J = 8 Hz, H_{arom}), 7.43 s (1H, H_{arom}), 7.46 t (2H, H_{arom}), 7.53 d (2H, J = 8.4 Hz, H_{arom}), 7.62 d (2H, J = 7.2 Hz, H_{arom}), 7.93 d (4H, J = 8.4 Hz, H_{arom}), 8.59 d (2H, J = 8.4 Hz, H_{arom}).

14-(3-Bromophenyl)-14*H*-dibenzo[*a*,*j*]xanthene (6j). White solid, mp 198–200°C. IR spectrum (KBr), ν, cm^{-1}: 3065, 2923, 1622, 1590, 1566, 1514, 1472, 1456, 1432, 1392, 1239. ^{1}H NMR spectrum, δ, ppm: 6.76 s (1H, 14-H), 7.11 t (1H, J = 7.6 Hz, H_{arom}), 7.17–7.19 m (1H, H_{arom}), 7.47 t (2H, J=7.2 Hz, H_{arom}), 7.57 d (2H, J = 8.8 Hz, H_{arom}), 7.63–7.67 m (3H, H_{arom}), 7.81 br.s (1H, H_{arom}), 7.94 d (4H, J = 8.8 Hz, H_{arom}), 8.70 d (2H, J = 8.4, H_{arom}).

Antibacterial activity. A liquid culture medium was prepared by adding 0.8 g of nutrient broth into 100 mL of distilled water, and test tubes were charged with 1 mL of the medium and autoclaved at 115°C for 15 min. Solutions of compounds **4** and **6** in DMSO at six concentrations of each sample were prepared (1000, 500, 250, 125, 62.5, and 31.25 μg/mL), and 1 mL of the solution was added to the autoclaved test tubes.

Standard bacterial cultures were diluted to a McFarland turbidity of 0.5, and 100 μL of the bacterial culture was added to each test tube. The test tubes were incubated overnight. The test tubes that appeared turbid were indicative of bacterial growth while tubes that remained clear indicated no growth. The MIC value was determined as the lowest concentration at which no bacterial growth was observed. Solutions of samples with a concentration corresponding to MIC and two higher concentrations were applied to MBC test. The concentration at which no bacterial growth was observed is reported as MBC.

CONFLICT OF INTEREST

The authors declare that they have no conflict of interest.

REFERENCES

1. Zolfigol, M.A., Nasrabadi, R.A., and Baghery, S., *Appl. Org. Chem*., 2016, vol. 30, p. 273. https://doi.org/10.1002/aoc.3428
2. Pasha, M.A. and Jayashankara, V.P., *Bioorg. Med. Chem. Lett*., 2007, vol. 17, p. 621. https://doi.org/10.1016/j.bmcl.2006.11.009
3. Sokolova, N.B., Lisina, I.V., and Tamoshauskas, N.A., *Russ. J. Appl. Chem*., 2011, vol. 84, p. 670. https://doi.org/10.1134/S1070427211040197
4. Huang, H., Yao, Y., Lin, Q., Zhao, J., Hua, C., and Gou, X., *Russ. J. Gen. Chem*., 2016, vol. 86, p. 934. https://doi.org/10.1134/S1070363216040307
5. Hanna, M.M., *Eur. J. Med. Chem*., 2012, vol. 55, p. 12. https://doi.org/10.1016/j.ejmech.2012.06.048
6. Shinde, S.V., Jadhav, W.N., and Karade, N.N., *Orient. J. Chem*., 2010, vol. 26, p. 307.
7. Karimi-Jaberi, Z. and Hashemi, M.M., *Monatsh. Chem*., 2008, vol. 139, p. 605. https://doi.org/10.1007/s00706-007-0786-z
8. Lichtner, R.B., Hutchinson, G., and Hellmann, K., *Eur. J. Cancer Clin. Oncol*., 1989, vol. 25, p. 945. https://doi.org/10.1016/0277-5379(89)90152-1
9. Casiraghi, G., Casnati, G., and Cornia, M., *Tetrahedron Lett.*, 1973, vol. 14, p. 679. https://doi.org/10.1016/S0040-4039(00)72432-4
10. Wang, J.Q. and Harvey, R.G., *Tetrahedron*, 2002, vol. 58, p. 5927. https://doi.org/10.1016/S0040-4020(02)00534-3
11. Jha, A. and Beal, J., *Tetrahedron Lett*., 2004, vol. 45, p. 8999. https://doi.org/10.1016/j.tetlet.2004.10.046
12. Kobayashi, S., Busujima, T., and Nagayama, S., *Chem. Eur. J*., 2000, vol. 6, p. 3491. https://doi.org/10.1002/1521-3765(20001002)6:19<3491::AID-CHEM3491>3.0.CO;2-P
13. Rostamizadeh, S., Shadjou, N., Amani, A.M., and Balalaie, S., *Chin. Chem. Lett*., 2008, vol. 19, p. 1151. https://doi.org/10.1016/j.cclet.2008.07.026
14. Soleimani, E., Khodaei, M.M., and Koshvandi, A.T.K., *Chin. Chem. Lett*., 2011, vol. 22, p. 927. https://doi.org/10.1016/j.cclet.2011.01.012
15. Gong, K., Fang, D., Wang, H.L., Zhou, X.L., and Liu, Z.L., *Dyes Pigm.*, 2009, vol. 80, p. 30. https://doi.org/10.1016/j.dyepig.2008.02.011
16. Hajipour, A.R., Ghayeb, Y., Sheikhan, N., and Ruoho, A.E., *Synlett*, 2010, vol. 2010, no. 5, p. 741. https://doi.org/10.1055/s-0029-1219399
17. Rahmatpour, A., *Monatsh. Chem*., 2011, vol. 142, p. 1259. https://doi.org/10.1007/s00706-011-0537-z
18. Ghassamipour, S. and Sardarian, A.R., *J. Heterocycl. Chem*., 2012, vol. 49, p. 669. https://doi.org/10.1002/jhet.780
19. Wang, J.Q. and Harvey, R.G., *Tetrahedron*, 2002, vol. 58, p. 5927. https://doi.org/10.1016/S0040-4020(02)00534-3
20. Stetter, H., *Newer Methods of Preparative Organic Chemistry*, Foerst, W., Ed., New York: Academic, 1963, vol. 2, p. 51. https://doi.org/10.1016/B978-0-12-395648-4.50010-6
21. Kumari, P., Yathindranath, V., and Chauhan, S.M.S., *Synth. Commun*., 2008, vol. 38, p. 637. https://doi.org/10.1080/00397910701798234
22. Tankam, T., Srisa, J., Sukwattanasinitt, M., and Wacharasindhu, S., *J. Org. Chem*., 2018, vol. 83, p. 11936. https://doi.org/10.1021/acs.joc.8b01824
23. Balakrishna, C., Kandula, V., Gudipati, R., Yennam, S., Devi, P.U., and Behera, M., *Synlett*, 2018, vol. 29, p. 1087. https://doi.org/10.1055/s-0036-1591898
24. Pourshamsian, K., *J. Chem. Health Risks*, 2018, vol. 8, p. 305. https://doi.org/10.22034/jchr.2018.544457
25. Montazeri, N., Pourshamsian, K., Rezaei, H., and Fouladi, M., *Asian J. Chem*., 2013, vol. 25, p. 3463. dx.doi.org/10.14233/ajchem.2013
26. Montazeri, N., Pourshamsian, K., Bayazi, M., and Kabiri, S., *Asian J. Chem*., 2013, vol. 25, p. 3373. https://doi.org/10.14233/ajchem.2013.13774
27. Montazeri, N., Pourshamsian, K., Yosefiyan, S., and Momeni, S.S., *J. Chem. Sci*., 2012, vol. 124, p. 883. https://doi.org/10.1007/s12039-012-0260-2
28. Yavari, I., Asgari, S.A., Pourshamsian, K., and Bagheri, M., *J. Sulfur Chem*., 2007, vol. 28, p. 477. https://doi.org/10.1080/17415990701471364
29. Tavakolifard, S., Biazar, E., Pourshamsian, K., and Moslemin, M.H., *Artif. Cells, Nanomed., Biotechnol*., 2016, vol. 44, p. 1247. https://doi.org/10.3109/21691401.2015.1019670

30. Jinxia, M., Wenhua, Z., Yajun, T., and Zhiguo, W., *Nanoscale Res. Lett.*, 2016, vol. 11, p. 200. https://doi.org/10.1186/s11671-016-1404-y
31. Darder, M., Aranda, P., and Ruiz-Hitzky, E., *Adv. Mater.*, 2007, vol. 19, p. 1309. https://doi.org/10.1002/adma.200602328
32. Seoyoun, S. and Jyongsik, J., *Chem. Commun.,* 2007, vol. 22, p. 4230. https://doi.org/10.1039/B707706H
33. Albadi, J., Mansournezhad, A., and Sadeghi, T., *Res. Chem. Intermed*., 2015, vol. 41, p. 8317. https://doi.org/10.1007/s11164-014-1894-0
34. Majid, M.H., Hamideh, A., Khadijeh, B., Mina, S., Hossein, A.O., and Fatemeh, F.B., *Bull. Chem. Soc. Ethiop*., 2011, vol. 25, p. 399. https://doi.org/10.4314/bcse.v25i3.68592
35. Shaterian, H.R., Doostmohammadi, R., and Ghashang, M., *Chin. J. Chem*., 2008, vol. 26, p. 338. https://doi.org/10.1002/cjoc.200890065
36. Fei-Oing, D., Li-Tao, A., and Jian-Ping, Z., *Chin. J. Chem*., 2007, vol. 25, p. 645. https://doi.org/10.1002/cjoc.200790120
37. Zakeri, M., Heravi, M., Saeedi, M., Karimi, N., Oskooie, H.A., and Tavakoli, N., *Chin. J. Chem*., 2011, vol. 29, p. 1441. https://doi.org/10.1002/cjoc.201180240
38. Wang, L.M., Sui, Y., and Zhang, L., *Chin. J. Chem*., 2008, vol. 26, p. 1105. https://doi.org/10.1002/cjoc.200890196
39. Yoshioka, E., Nishimura, M., Nakazawa, T., Kohtani, S., and Miyabe, H., *J. Org. Chem*., 2015, vol. 80, p. 8464. https://doi.org/10.1021/acs.joc.5b01452
40. Zang, H., Zhang, Y., Cheng, B., Zhang, W., Xu, X., and Ren, Y., *Chin. J. Chem*., 2012, vol. 30, p. 362. https://doi.org/10.1002/cjoc.201180488
41. Yuling, L., Baixiang, D.U., Xiaoping, X.U., Daqing, S.H.I., and Shunjun, J.I., *Chin. J. Chem*., 2009, vol. 27, p. 1563. https://doi.org/10.1002/cjoc.200990264